2007-09

Enhancement of the daytime MODIS based icing potential using COAMPS and NOGAPS model data

Davidson, Richard Lee

Monterey, California. Naval Postgraduate School

NAVAL POSTGRADUATE SCHOOL

MONTEREY, CALIFORNIA

THESIS

ENHANCEMENT OF THE DAYTIME MODIS BASED ICING POTENTIAL USING COAMPS AND NOGAPS MODEL DATA

by

Richard Lee Davidson

September 2007

Thesis Advisor:	Philip Durkee
Second Reader:	Kurt Nielsen

Approved for public release; distribution is unlimited.

THIS PAGE INTENTIONALLY LEFT BLANK

REPORT DOCUMENTATION PAGE			Form Approved OMB No. 0704-0188
Public reporting burden for this collection of information is estimated to average 1 hour per response, including the time for reviewing instruction, searching existing data sources, gathering and maintaining the data needed, and completing and reviewing the collection of information. Send comments regarding this burden estimate or any other aspect of this collection of information, including suggestions for reducing this burden, to Washington headquarters Services, Directorate for Information Operations and Reports, 1215 Jefferson Davis Highway, Suite 1204, Arlington, VA 22202-4302, and to the Office of Management and Budget, Paperwork Reduction Project (0704-0188) Washington DC 20503.			
1. AGENCY USE ONLY *(Leave blank)*	**2. REPORT DATE** September 2007	**3. REPORT TYPE AND DATES COVERED** Master's Thesis	
4. TITLE AND SUBTITLE Enhancement of the Daytime MODIS Based Icing Potential Using NOGAPS and COAMPS Model Data		**5. FUNDING NUMBERS**	
6. AUTHOR(S) Richard L. Davidson			
7. PERFORMING ORGANIZATION NAME(S) AND ADDRESS(ES) Naval Postgraduate School Monterey, CA 93943-5000		**8. PERFORMING ORGANIZATION REPORT NUMBER**	
9. SPONSORING /MONITORING AGENCY NAME(S) AND ADDRESS(ES) N/A		**10. SPONSORING/MONITORING AGENCY REPORT NUMBER**	
11. SUPPLEMENTARY NOTES The views expressed in this thesis are those of the author and do not reflect the official policy or position of the Department of Defense or the U.S. Government.			
12a. DISTRIBUTION / AVAILABILITY STATEMENT Approved for public release; distribution is unlimited.		**12b. DISTRIBUTION CODE**	

13. ABSTRACT (maximum 200 words)

In this thesis, NOGAPS and COAMPS model data are fused with Alexander (2005) algorithm to determine its usefulness in enhancing satellite-based aircraft icing analysis. This is a follow on to Cooper (2006) research where MM5 and ETA were used. Using historical NOGAPS and COAMPS data (T, Td and RH) accessed from the GODAE server, several storms from 2004 were fused with available MODIS imagery from the same storms to produce an enhanced icing product. Pilot reports (PIREPS) were used as a validation tool to determine where icing was taking place during the storms analyzed. A comparison was made between the MODIS-based icing potential and the model-based icing potential. The two icing potentials were fused together to produce an enhanced icing product. Statistical analysis using ROC curves was performed on the various combinations to determine which product combination gave the best results. Two different available T_{map} (Alexander and CIP) were used and had mixed results. Contrary to what Cooper (2006) found where weighting RH and the Alexander T_{map} produced the best results; this study found that equal weighting of T and RH and the CIP T_{map} produced the same or better results than weighting RH. This study also found that NOGAPS combined with the MODIS algorithm provide the best icing potential results.

14. SUBJECT TERMS MODIS, icing, UAV, NOGAPS, COAMPS, ROC, PIREPS, multispectral satellite analysis	**15. NUMBER OF PAGES** 57
	16. PRICE CODE

17. SECURITY CLASSIFICATION OF REPORT	**18. SECURITY CLASSIFICATION OF THIS PAGE**	**19. SECURITY CLASSIFICATION OF ABSTRACT**	**20. LIMITATION OF ABSTRACT**
Unclassified	Unclassified	Unclassified	UU

NSN 7540-01-280-5500 Standard Form 298 (Rev. 2-89)
Prescribed by ANSI Std. 239-18

THIS PAGE INTENTIONALLY LEFT BLANK

Approved for public release; distribution is unlimited.

ENHANCEMENT OF THE DAYTIME MODIS BASED ICING POTENTIAL USING NOGAPS AND COAMPS MODEL DATA

Richard L. Davidson
Lieutenant, United States Navy
B.S., The Citadel, 2001

Submitted in partial fulfillment of the
requirements for the degree of

MASTER OF SCIENCE IN PHYSICAL OCEANOGRAPHY AND METEOROLOGY

from the

NAVAL POSTGRADUATE SCHOOL
September 2007

Author: Richard L. Davidson

Approved by: Philip A. Durkee
Thesis Advisor

Kurt Nielsen
Second Reader

Philip A. Durkee
Chairman, Department of Meteorology

THIS PAGE INTENTIONALLY LEFT BLANK

ABSTRACT

In this thesis, NOGAPS and COAMPS model data are fused with Alexander (2005) algorithm to determine its usefulness in enhancing satellite-based aircraft icing analysis. This is a follow on to Cooper (2006) research where MM5 and ETA were used. Using historical NOGAPS and COAMPS data (T, Td and RH) accessed from the GODAE server, several storms from 2004 were fused with available MODIS imagery from the same storms to produce an enhanced icing product. Pilot reports (PIREPS) were used as a validation tool to determine where icing was taking place during the storms analyzed. A comparison was made between the MODIS-based icing potential and the model-based icing potential. The two icing potentials were fused together to produce an enhanced icing product. Statistical analysis using ROC curves was performed on the various combinations to determine which product combination gave the best results. Two different available T_{map} (Alexander and CIP) were used and had mixed results. Contrary to what Cooper (2006) found where weighting RH and the Alexander T_{map} produced the best results; this study found that equal weighting of T and RH and the CIP T_{map} produced the same or better results than weighting RH. This study also found that NOGAPS combined with the MODIS algorithm provide the best icing potential results.

THIS PAGE INTENTIONALLY LEFT BLANK

TABLE OF CONTENTS

LIST OF FIGURES

THIS PAGE INTENTIONALLY LEFT BLANK

LIST OF TABLES

THIS PAGE INTENTIONALLY LEFT BLANK

ACKNOWLEDGMENTS

The author would like to thank Professor Durkee for his guidance during the thesis process and Kurt Nielsen for serving as second reader. Jeremy Alexander made this thesis possible with his algorithm design and Michael Cooper followed on with his MM5 data to enhance the MODIS product which paved the way for my COAMPS and NOGAPS product. Mary Jordan was crucial in compiling the MATLAB code and getting my thesis started. Thanks to Dan Geiszler and Rodney Jacques for their knowledge and wisdom about COAMPS and models in general. Tom Neu and the FNMOC staff bent over backwards to provide COAMPS data in real time and went out of their way to insure I got the data I needed. CDR Stone provided some crucial model insight and was the one that suggested NOGAPS should be included and provided the information about the GODAE server.

A special thanks to my parents who have supported me at every turn of my career and a very big thanks to my wife and children who have supported me during this long and arduous process.

THIS PAGE INTENTIONALLY LEFT BLANK

I. INTRODUCTION

A. BACKGROUND

The military is becoming more dependent on remotely operated aircraft, known as unmanned aerial vehicles (UAV), and precision guided land attack missiles. While this minimizes the risk to human life, there are still risks that are shared with manned aircraft such as in-flight icing. Icing is important because "[i]t destroys the smooth flow of air, increasing drag while decreasing the ability of the airfoil to create lift" (AOPA 2002). Ice that has accreted on a wing is depicted in Figure 1.

Figure 1. Ice accreted on wing from (From Hearn 2007)

The disruption of air over the airfoil can eventually lead to a stall and possible crash. It is impossible to avoid icing situations unless all flight operations are cancelled, which is unreasonable in both civilian and military operations, but icing can be mitigated with good forecasting and aircraft mounted deicing equipment.

B. MOTIVATION

Aircraft mounted deicing equipment can not be relied upon in extreme icing conditions and in some cases can not be operated continuously. Therefore, it is extremely important that the pilot/UAV operator know about potential icing situations so they can insure their equipment is operating correctly and possibly avoid the potential icing areas. This is a daunting task given that some UAV missions exceed 24 hours in length and some may even approach 48 hours. The possibility of a two day mission is where the forecaster must have the best available tools at their disposable. There has already been a loss of several RQ-1 Predators' (UAV) due to icing (Kilian 2001). Land attack missiles and other precision munitions can be susceptible to icing and are often launched over areas where there is limited meteorological data. Lack of meteorological data and extended forecasts require that a forecaster use more than thumb rules for icing calculations.

Forecasters in the United States, both civilian and military, seem to have a good handle on forecasting icing potential. Part of their success stems from the detailed meteorological observations available including remote sensing from radars and satellites. The current icing potential (CIP) product from the National Weather Service (NWS) uses a combination of products such as model output, radar, satellite and pilot reports to produce the best available current icing potential. Unfortunately, the areas where the military operates typically do not have meteorological radar coverage or pilot reports. This means that the forecasters must rely on model output and satellite data. Currently, most forecasters rely on the model temperature (T) and relative humidity (RH) fields to determine icing potential. This method results in large areas of potential icing where actual icing may not be occurring. While this provides the greatest safety cushion, it limits the planning of military missions and possibly jeopardizes time-sensitive

operations. Alexander (2005) showed that MODIS imagery could be used to predict icing potential and Cooper (2006) showed that the MODIS icing potential could be fused with model data, specifically ETA and MM5, to produce a better CIP product. This fused icing product would be very helpful to all military planners. Unfortunately, the military services, specifically the United States Air Force (USAF) and United States Navy (USN), use their own models due to their different operational environments. The USN conducts many of their operations over water and relies on the NOGAPS and COAMPS models so a different study is needed to see if the same benefits can be obtained using NOGAPS and COAMPS that Cooper (2006) found for the MM5.

C. PURPOSE

The purpose of this research is to improve upon the Alexander (2005) MODIS 9-channel fuzzy logic icing algorithm using NOGAPS and COAMPS model data. Alexander (2005) showed that the MODIS icing algorithm did a better job than the current GOES icing algorithm mainly due to the increase in available satellite channels. Cooper (2006) fused the MODIS icing algorithm output with model data to produce a better CIP product than the MODIS icing algorithm alone. This research will be a follow on to Cooper (2006) research using NOGAPS and COAMPS model data and determine if the USN's operational models improve upon Alexander's MODIS icing algorithm.

D. THESIS PLAN

Using historical pilot reports (PIREPS) some major icing events were identified from January 2004. NOGAPS and COAMPS historical data from the Global Ocean Data Assimilation Experiment (GODAE) were downloaded in GRIB format and decoded. This data was fused with MODIS imagery that has been processed with Alexander (2005) MODIS icing algorithm. Using the historical PIREPS, statistics were produced to determine what value if any is added from the model data to the MODIS icing algorithm. It is possible that the value added will change with various meteorological situations and it must be determined if having a forecaster in the loop (FITL) will be needed to analyze the output vice relying on straight automation of the process. The theory will be

discussed in Chapter II. Chapter III will cover the data collection and verification process. In Chapter IV the results will be revealed followed by conclusion and recommendations in Chapter V.

II. THEORY

A. MODIS BASED ICING POTENTIAL ALGORITHM

Using nine of the 36 MODIS channels Alexander (2005) constructed an algorithm that used fuzzy logic over a series of twelve tests to produce an icing potential. The twelve tests were broken up into four groups and listed in Table 1 below. The tests are thoroughly explained in Alexander (2005), to a lesser extent in Cooper (2006) and will only be briefly explained here.

Table 1. MODIS Icing Test (From Alexander 2005)

Test Group	Test (no units unless noted)	Icing Reflectance Thresholds
I	0.65 μm Reflectance (P01)	Min < 0.10 Max >0.25
I	1.63 μm Reflectance (P06)	> 0.5
I	2.10 μm Reflectance (P07)	> 0.4
I	3.90 μm Reflectance (P22)	> 0.06
I	Cirrus Reflectance (P26)	< 0.08
II	1.63 μm Ratio (P61)	Min < 0.2 Max >0 .9
II	2.10 μm Ratio (P71)	Min < 0.15 Max > 0.65
III	Temperature (C) (P31)	Min > 0 & < -40 Max=-10
IV	3.9-11 μm BTD (C) (BTD1)	> 10 (Day)
IV	8-11 μm BTD (C) (BTD2)	Min > 3 Max< -2
IV	11-12 μm BTD (C) (BTD3)	< -0.5 & > 4.5
IV	Trispectral BTD (C)(BTD4)	Same as 8-11 μm BTD

1. Group I Reflectance Tests

Reflectance is simply a measurement of the amount of energy that is received at the satellite after being reflected by a surface. Alexander uses Channels 1 (0.65μm), 6 (1.6μm), 7 (2.1μm), 22 (3.9μm) and 26 (1.38μm), which due to their wavelength interact with the cloud particles, to help separate clouds from the background land or ocean. Channels 6, 7 and 26 can be used to determine cloud phase because of their scattering property differences. Channel 26 whose wavelength is strongly absorbed by water vapor can look for ice clouds where the temperature is so cold there is little or no chance of icing.

a. P01 Reflectance Test

Using MODIS channel 1 clouds can be distinguished from ground or ocean, but this is more difficult if the ground is desert or snow/ice covered. Thick clouds will have a very high reflectance and the icing probability as a function of channel 1 reflectance is shown in Figure 2.

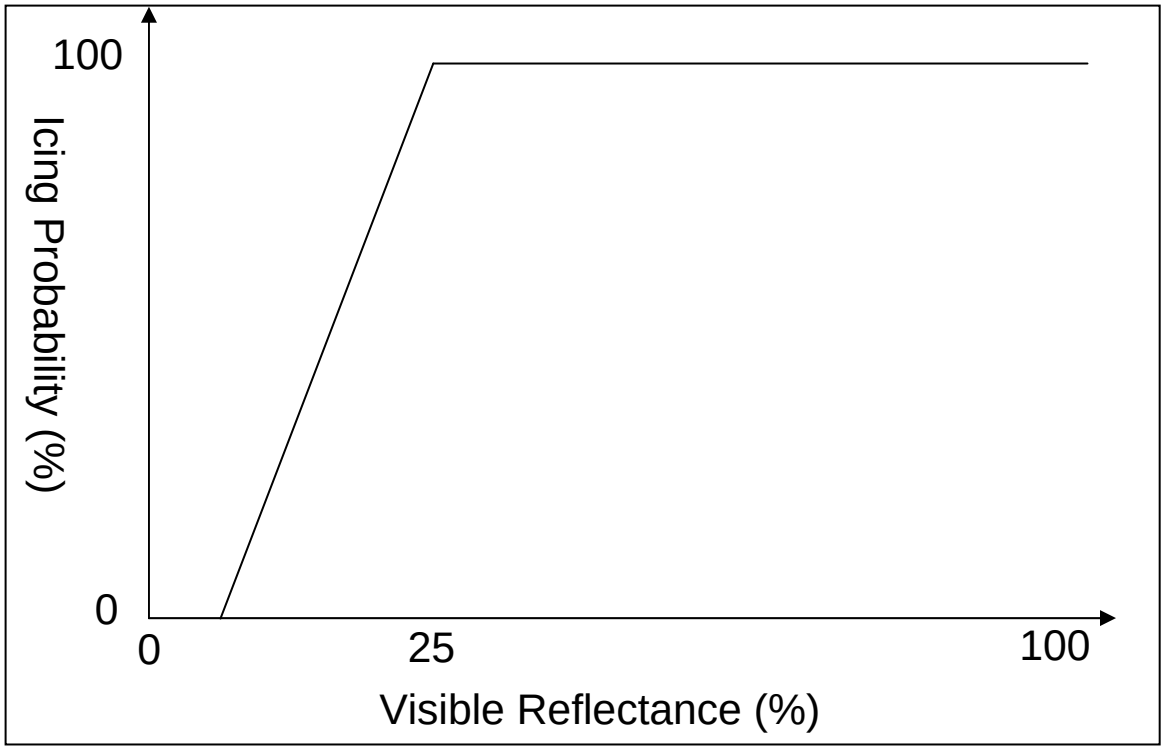

Figure 2. P01 icing potential vs. CH 1 reflectance percentage (From Alexander 2005)

b. P06 Reflectance Test

Using MODIS channel 6 the phase of the cloud can be determined. While the real indices of refraction are nearly equal at the 1.63 μm wavelength looking at Figure 3 below one can see that imaginary indices of refraction are significantly different for ice and water. It is this difference that allows for phase determination. Figure 4 illustrates the icing potential as a function of the channel 6 reflectance.

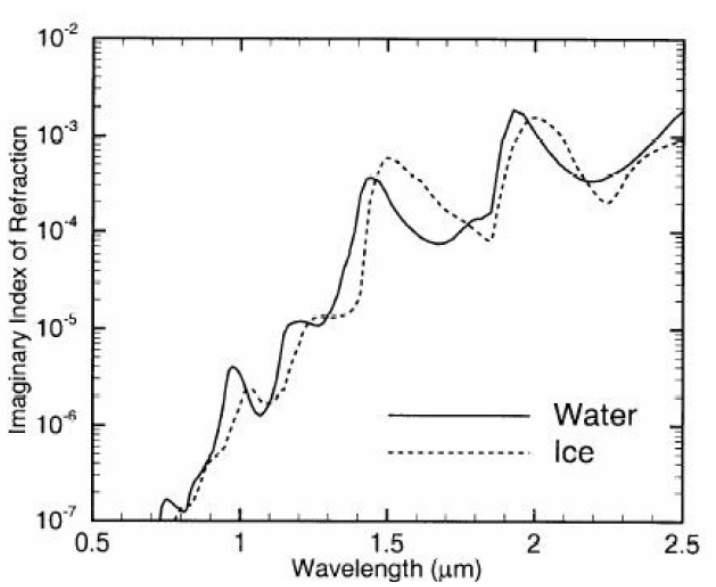

Figure 3. Imaginary Index of refraction between 0.5 μm and 2.5 μm (From Braum et al. 2000)

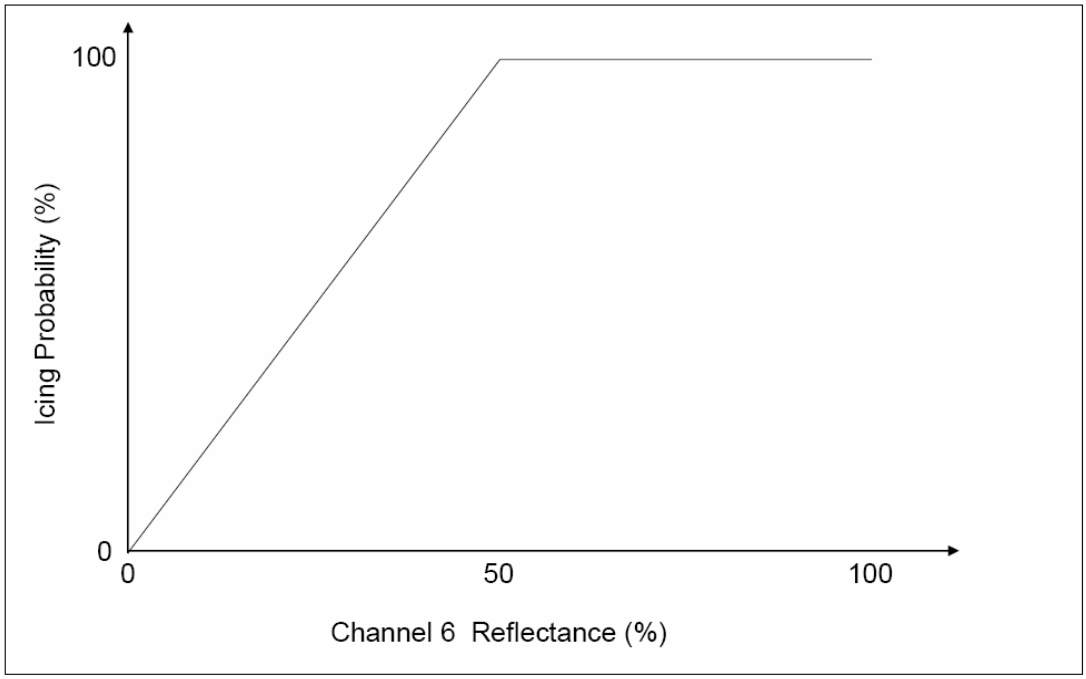

Figure 4. P06 icing potential vs. CH 6 reflectance percentage (From Alexander 2005)

c. P07 Reflectance Test

The P07 reflectance test is very similar to the P06 test except the imaginary index of refraction between water and ice is slightly less. Figure 5 shows icing potential as a function of channel 7 reflectance.

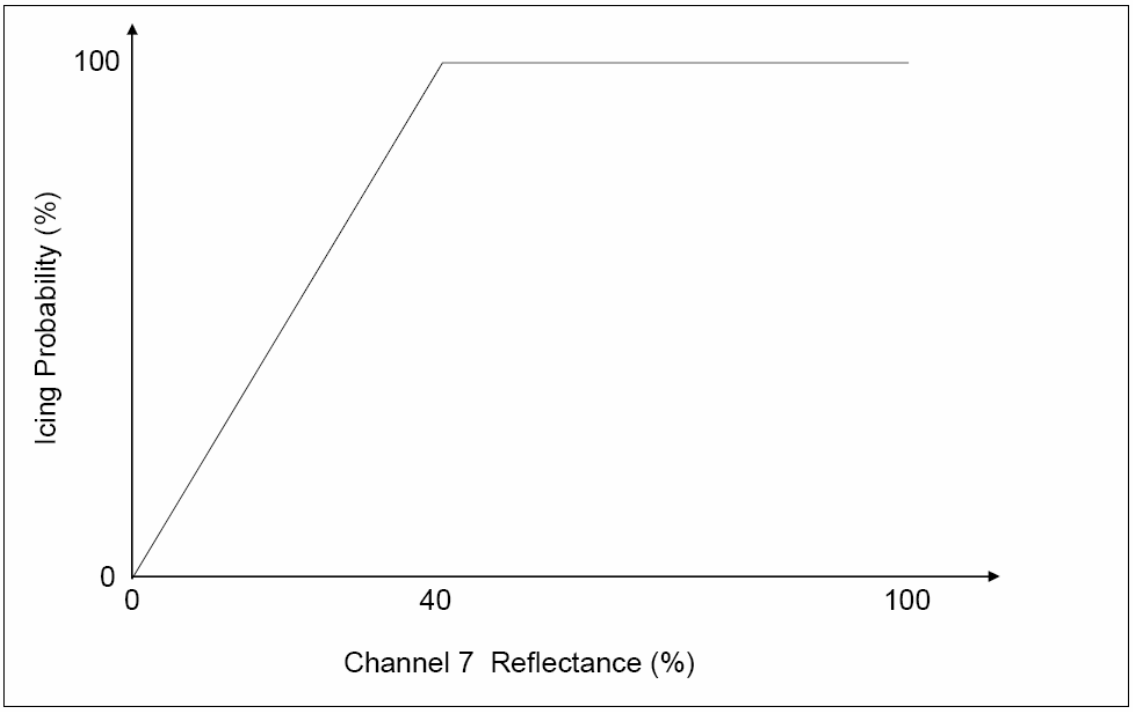

Figure 5. P07 icing potential vs. CH 7 reflectance percentage (From Alexander 2005)

d. P22 Reflectance Test

The P22 reflectance test takes place in the transition zone (3.9 μm wavelength) between the satellite sensing incoming solar radiation and outgoing terrestrial radiation. Because water clouds reflect more energy than ice clouds once again phase can be determined. Figure 6 shows icing potential as a function of channel 22 reflectance.

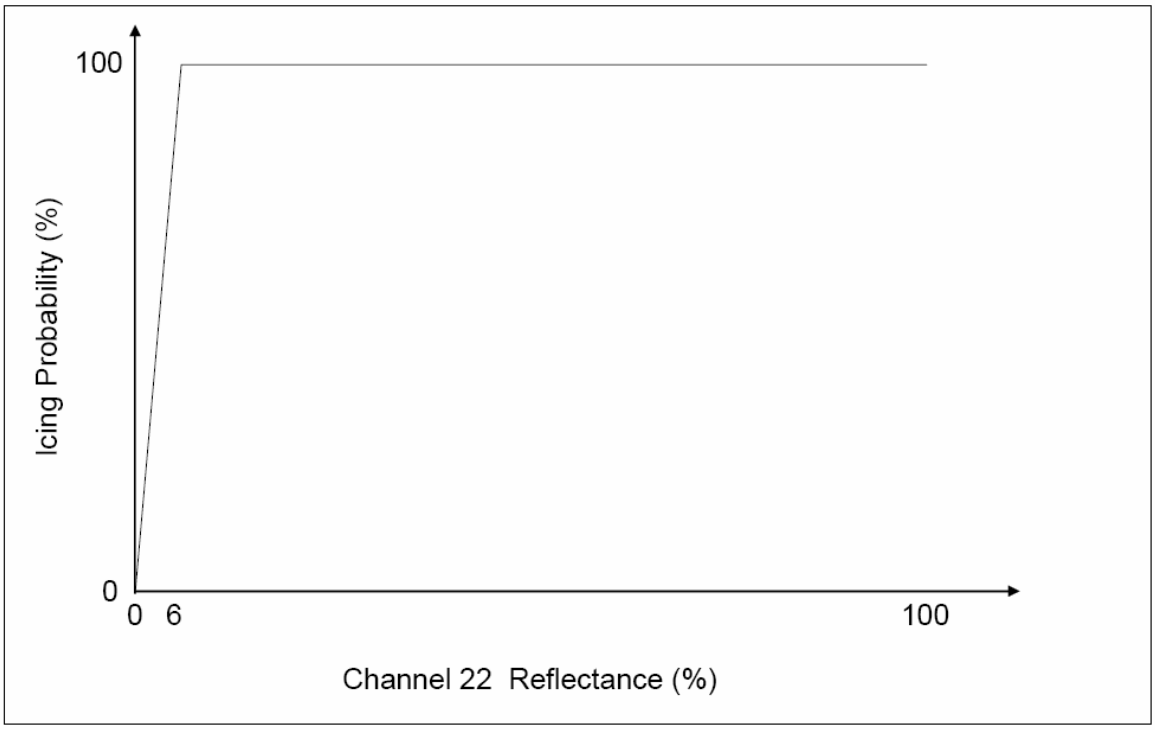

Figure 6. P22 icing potential vs. CH 22 reflectance percentage (From Alexander 2005)

e. P26 Reflectance Test

This test differs from the previous tests because it is not determining where the icing potential is high, but where there is no or very little icing potential. Figure 7 illustrates icing potential as a function of channel 26 reflectance.

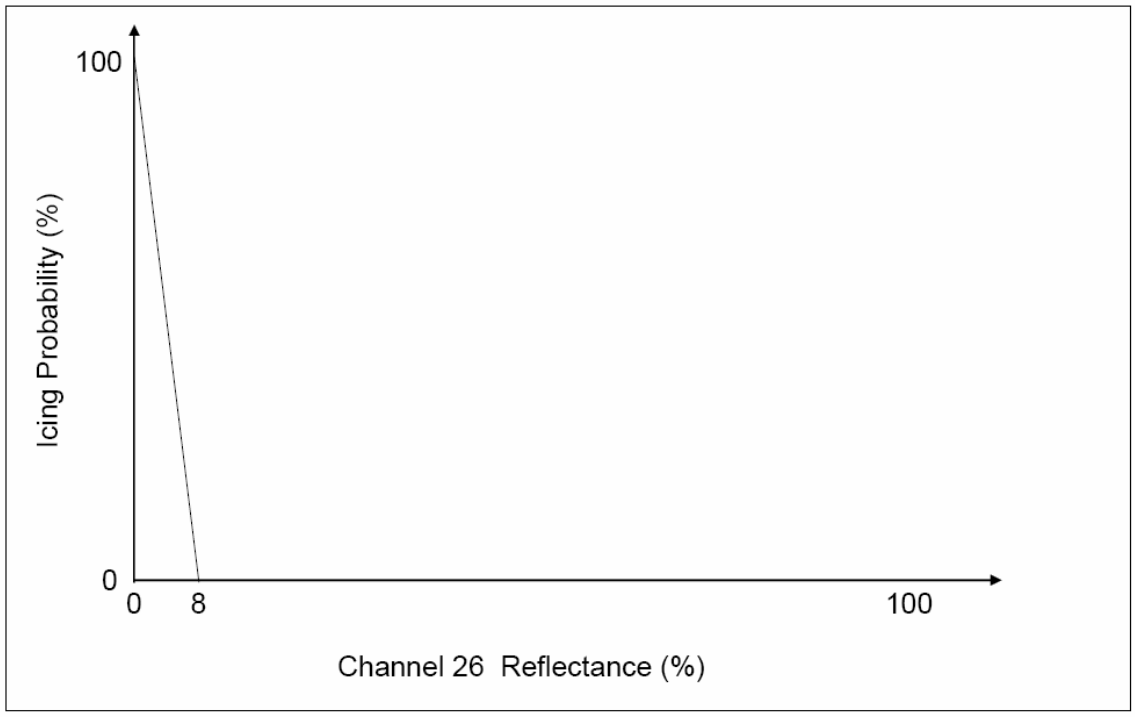

Figure 7. P26 icing potential vs. CH 26 reflectance percentage (From Alexander 2005)

2. Group II Reflectance Tests

The Group II reflectance tests are ratio tests that are better suited for determining phase than the Group I tests alone. Channels 1, 6 and 7 were used from the Group I tests and two ratios were determined; channel 6 to channel 1 (P61) and channel 7 to channel 1 (P71). Water clouds will have a higher reflectance than ice clouds and since supercooled liquid water (SLW) is a major factor in icing and would exhibit a high ratio for channels sensitive to cloud phase. As shown in Figure 8 for P61 and Figure 9 for P71 icing probability increases sharply for Channel 6 at 60% reflectance ratio and is 100% icing probability when the ratio is 90% and greater. Icing probability follows a similar pattern for Channel 7, but the sharp increase is at 35% and is 100% icing probability when the ratio is 65%.

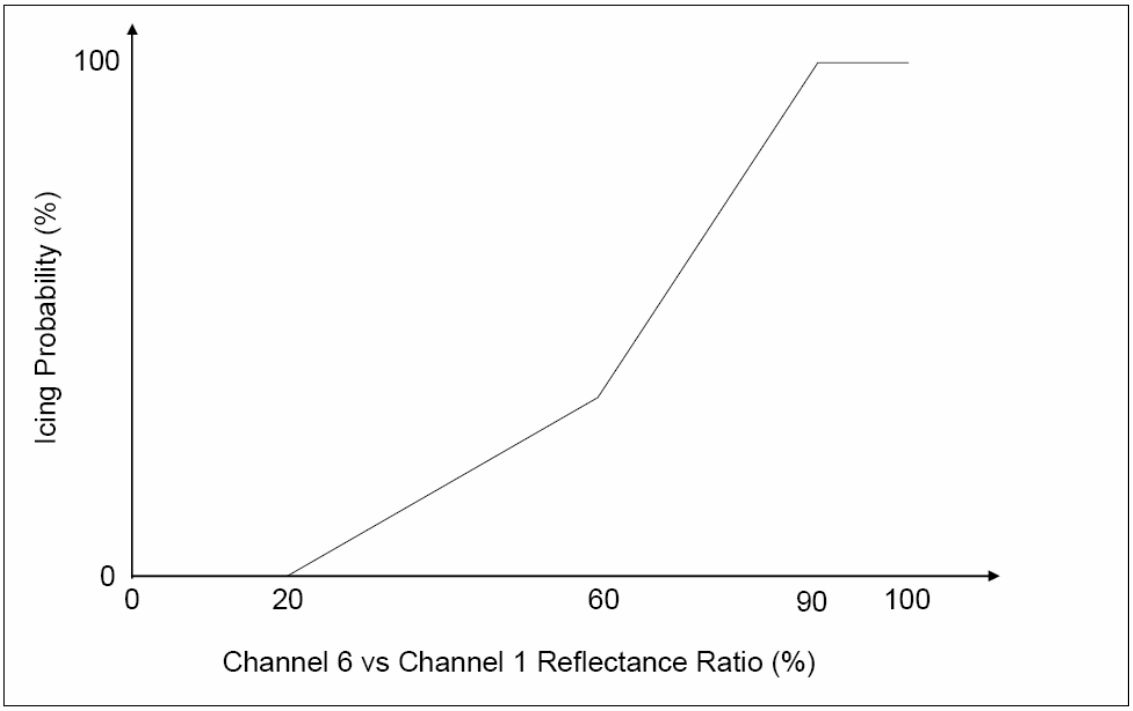

Figure 8. P61 icing potential vs. P61 ratio (From Alexander 2005)

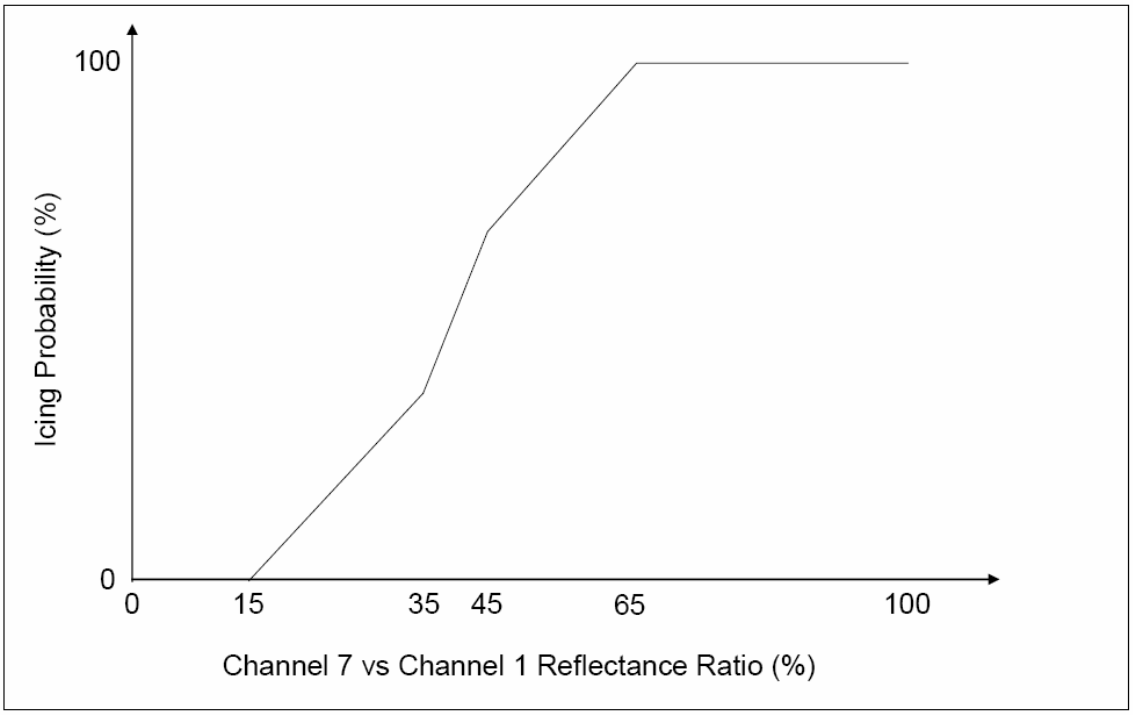

Figure 9. P71 icing potential vs. P71 ratio (From Alexander 2005)

3. Group III Brightness Temperature Test (P31)

MODIS channel 31 covers the 11 μm wavelength and at this wavelength clouds are both good absorbers and good emitters. The earth's radiation at this wavelength is absorbed and emitted by the clouds. Because the satellite is sensing the top few meters of the clouds, the cloud top temperature can be accurately ascertained and the remaining cloud temperature can be assumed to be warmer. Figure 10 illustrates icing probability as a function of that brightness temperature.

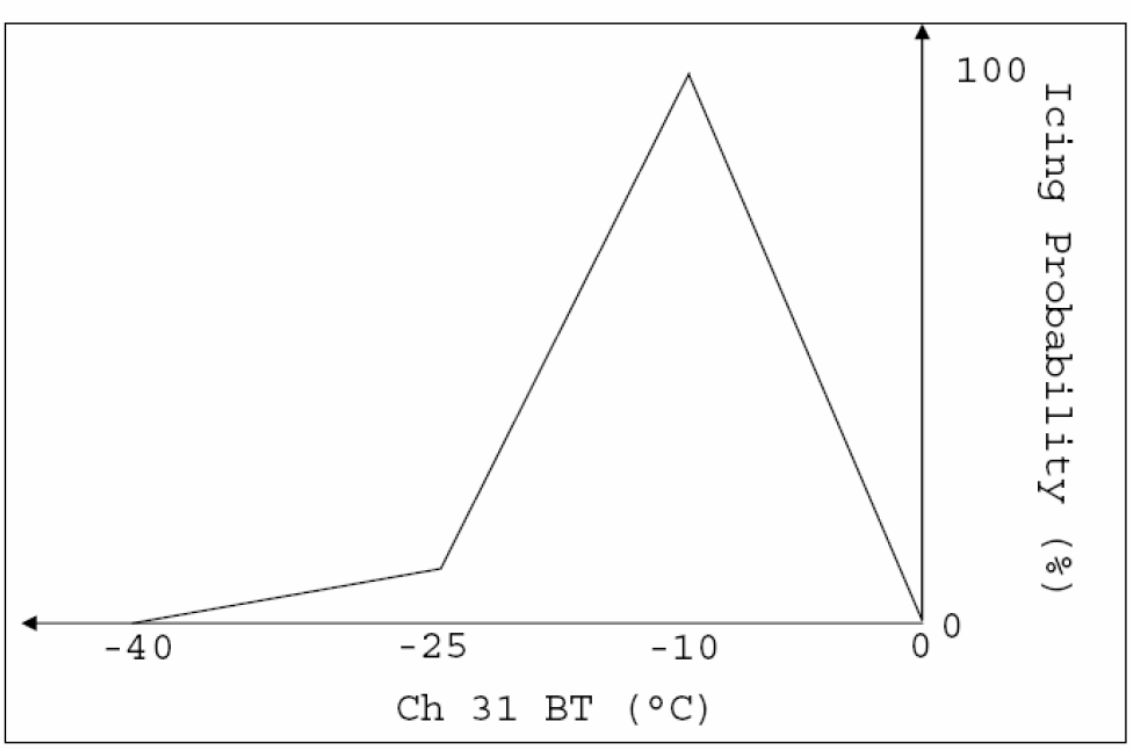

Figure 10. P31 brightness temperature probability values (From Alexander 2005)

4. Group IV Brightness Temperature Difference Tests

The Group IV tests are used for phase differentiation within the clouds by using the difference in imaginary index of refraction for water and ice from one wavelength to the next. The brightness temperature will change as the wavelength changes and that change can exploited for the differences between water and ice.

a. BTD1 Brightness Temperature Difference Test

During daylight hours channel 22 will have a higher brightness temperature than channel 31 because at the channel 22 wavelength, energy is reflected and emitted by the clouds (Cooper 2006). If it is a water cloud the difference will even be greater since water clouds have a higher reflectance at the channel 22 wavelength. Figure 11 shows that as the difference between channel 22 and channel 31 becomes larger the icing potential also becomes greater.

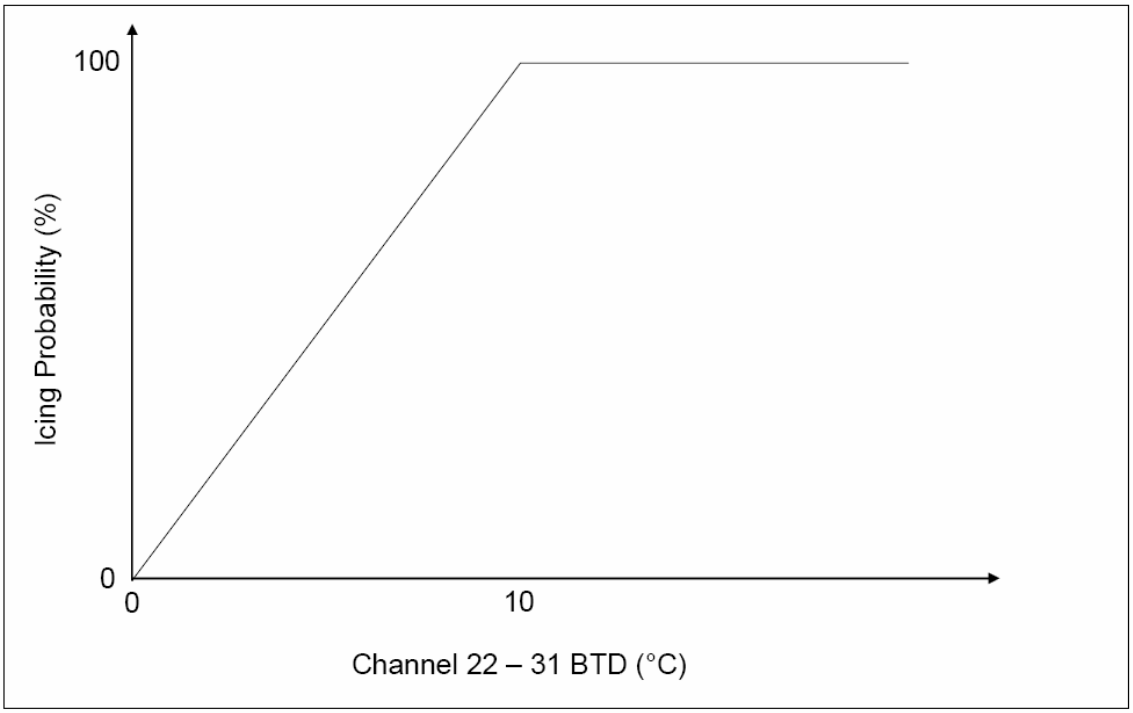

Figure 11. BTD1 icing potential vs. CH 22-31 brightness temperature difference (From Alexander 2005)

b. BTD2 Brightness Temperature Difference Test

The BTD2 brightness temperature difference test is slightly different from the previous tests since it can produce a negative value. The test is based on taking the brightness temperature difference between channels 29 and 31. The difference can produce a negative value since the absorption coefficient for water and ice are the same

for channel 29, but increases in channel 31 for ice. Water clouds will produce a negative value and ice clouds a positive value. The icing probability as a function of the difference is shown in Figure 12.

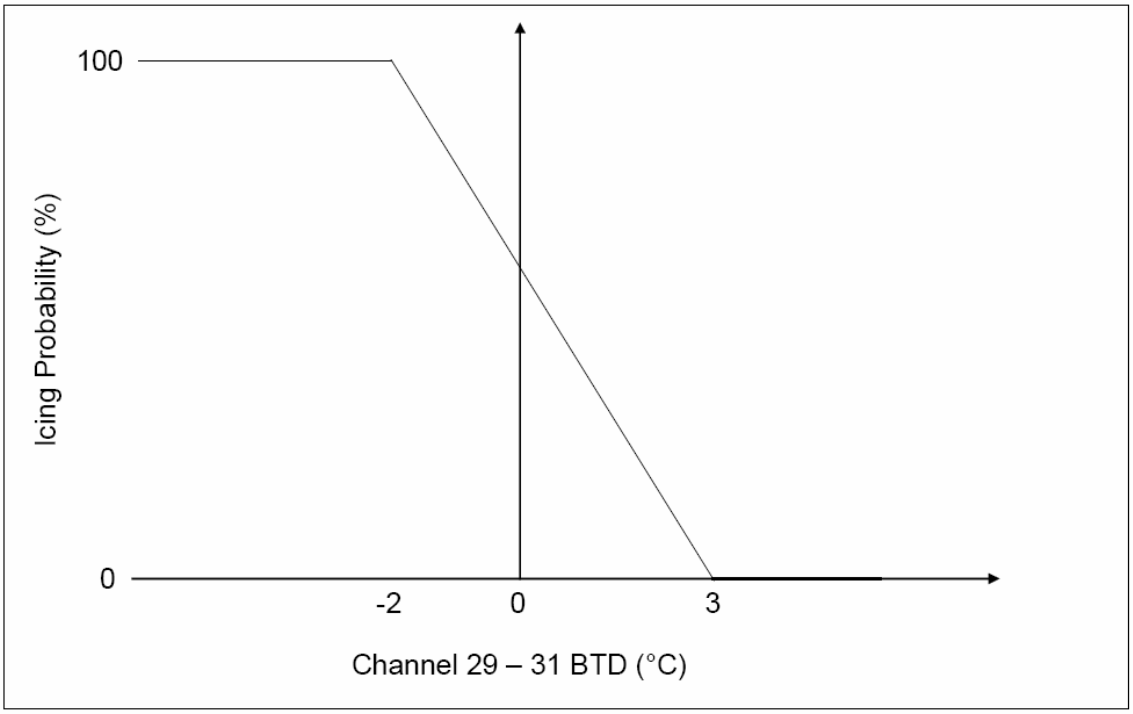

Figure 12. BTD2 icing potential vs. CH 29-31 brightness temperature difference (From Alexander 2005)

c. BTD3 Brightness Temperature Difference Test

BTD3 brightness temperature difference is somewhat similar to BTD 2, but its main purpose is to identify cirrus clouds. Figure 13 shows the band, 0.8-1.5, where cirrus would be likely.

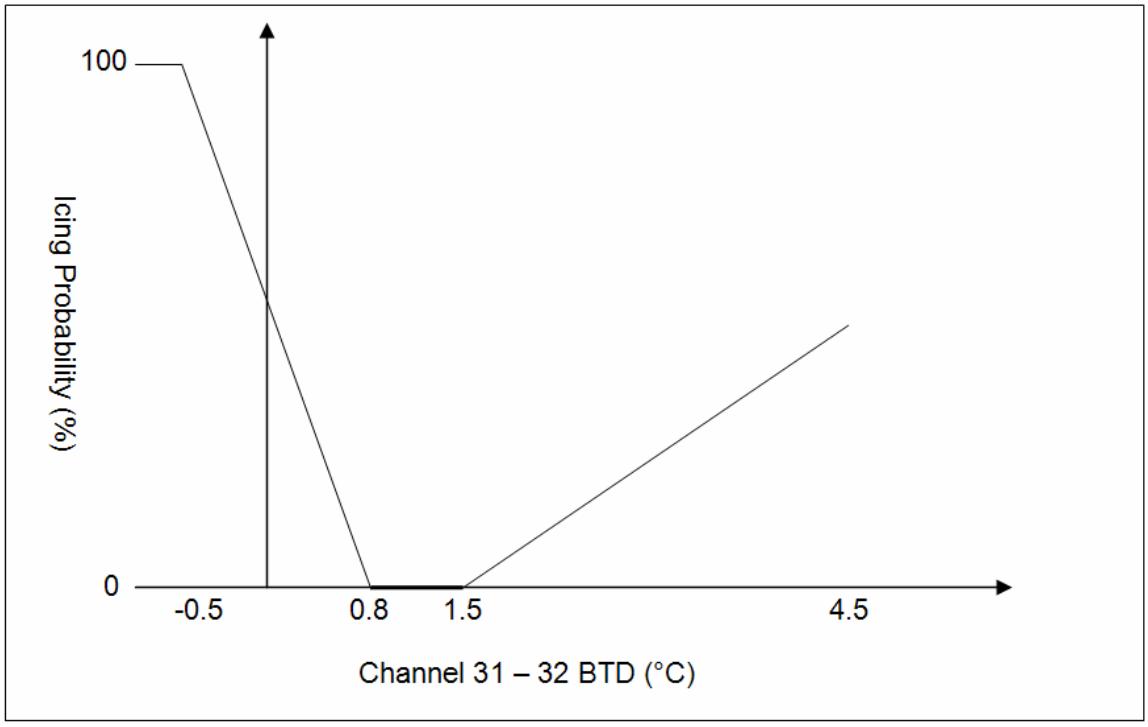

Figure 13. BTD3 icing potential vs. CH 31-32 brightness temperature difference (From Alexander 2005)

d. BTD4 Trispectral Brightness Temperature Difference Test

The trispectral brightness temperature difference test is the difference between BTD2 and BTD3. Due to their temperature difference relations, if it is a water cloud BTD2 would be negative and BTD3 would be positive resulting in a large negative number. If there is good mixture of water and ice clouds the value will be closer to zero. If it is strictly an ice cloud the value will be positive. Figure 14 shows the icing potential as a function of the BTD2 and BTD3 difference.

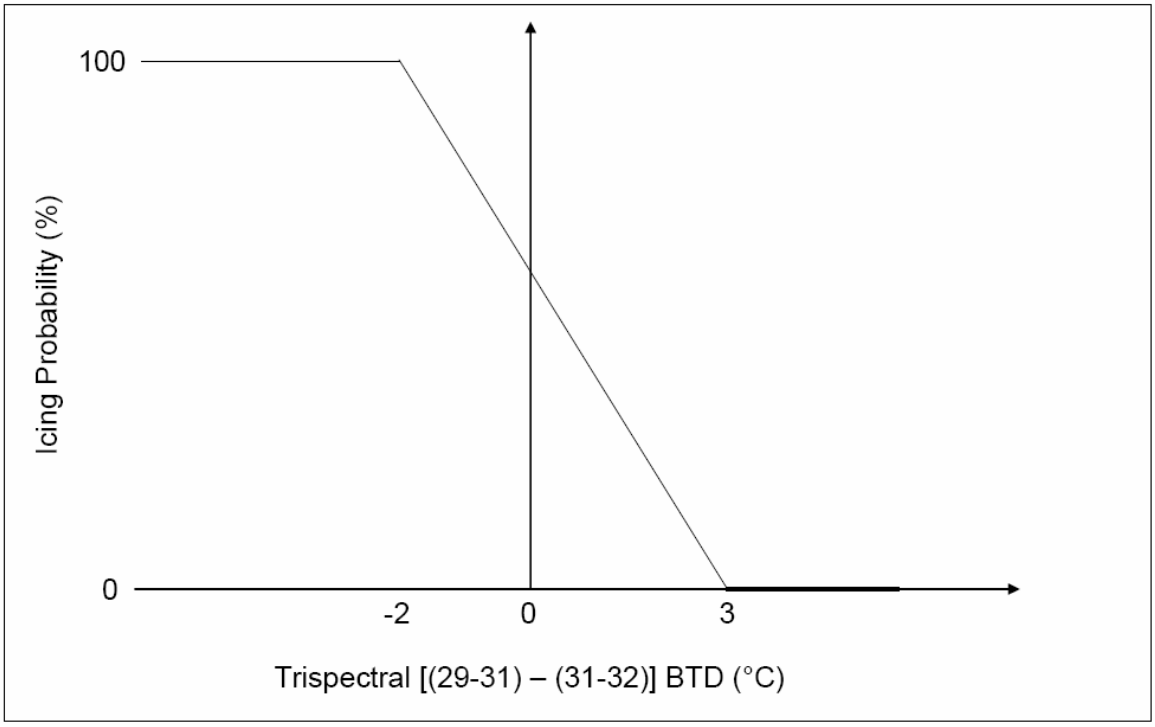

Figure 14. BTD4 icing potential vs. trispectral brightness temperature difference (From Alexander 2005)

5. Final MODIS Algorithm Test

The final MODIS algorithm test is a simple mathematical function that takes the highest value for each pixel of each group and multiplies the four groups together and then the fourth root is taken to determine the final icing potential. A flowchart of the algorithm is shown in Figure 15.

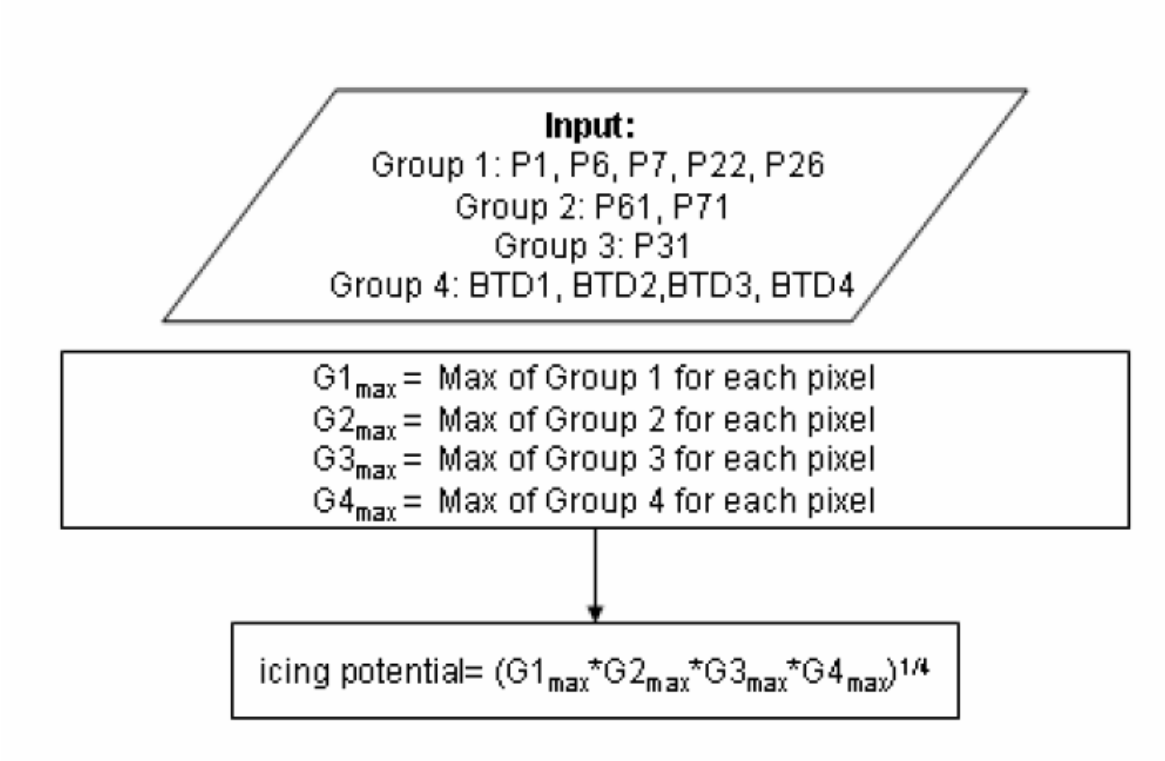

Figure 15. Flowchart for the final MODIS algorithm test (From Cooper 2006)

B. MODEL BASED ICING POTENTIAL DETERMINATION

Model determination of icing in its simplest form involves answering two questions: Where are the clouds and where in the clouds is it conducive to icing? The simplest two model parameters that answer those two questions are temperature and relative humidity. There have been several studies done to answer at what RH are cloud formations likely. While the top number of 100% is a given it is the lower threshold where the debate lies. Looking at Figure 16 one can see that icing can occur as low as 30% RH. Relative Humidity of 60% and greater is a common assumption for cloud formation. Using the RH based Interest Map in Figure 16 allows the use of fuzzy logic where the higher RH's are weighted heavier than the lower ones.

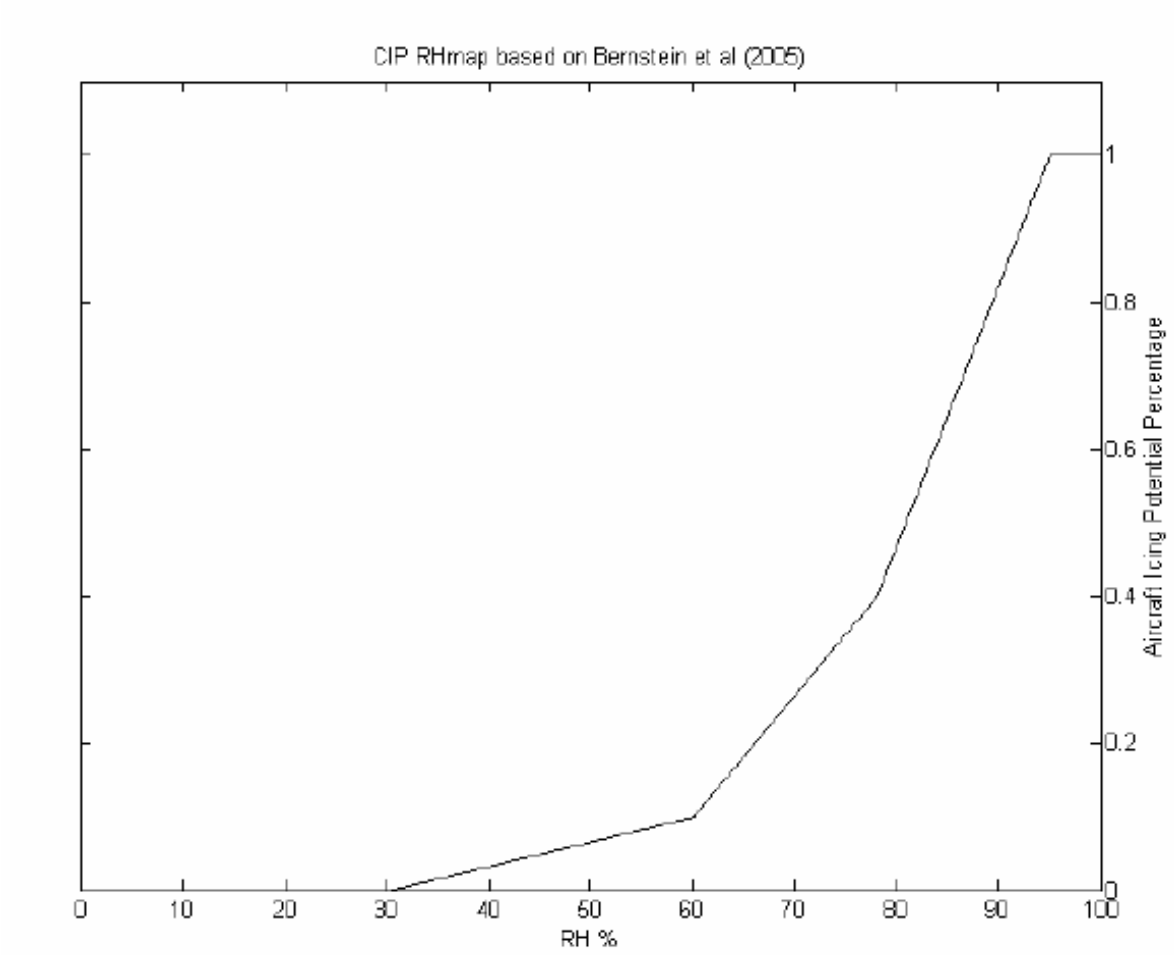

Figure 16. Icing potential as a function of relative humidity (From Bernstein et al. 2005)

The second piece needed for icing potential is temperature. The upper limit of 0C is a given, but the lower limit and where icing peaks is open for discussion. For the lower limit, it is known that between SLW begins to instantaneously freeze between -25C and -40C there is no longer an icing threat. The two T Interest Maps used in this study and Cooper's similar study, shown in Figure 17, show different peaks and different tails for the lower limits. Alexander's T Interest Map has a distinct peak, but the CIP developed by Bernstein et al. has a peak over a range of values which gives a higher icing probability over a broader range of temperatures. The results section will illustrate which one was more successful in this study.

Using the T and RH Interest Maps together an icing probability can be determined.

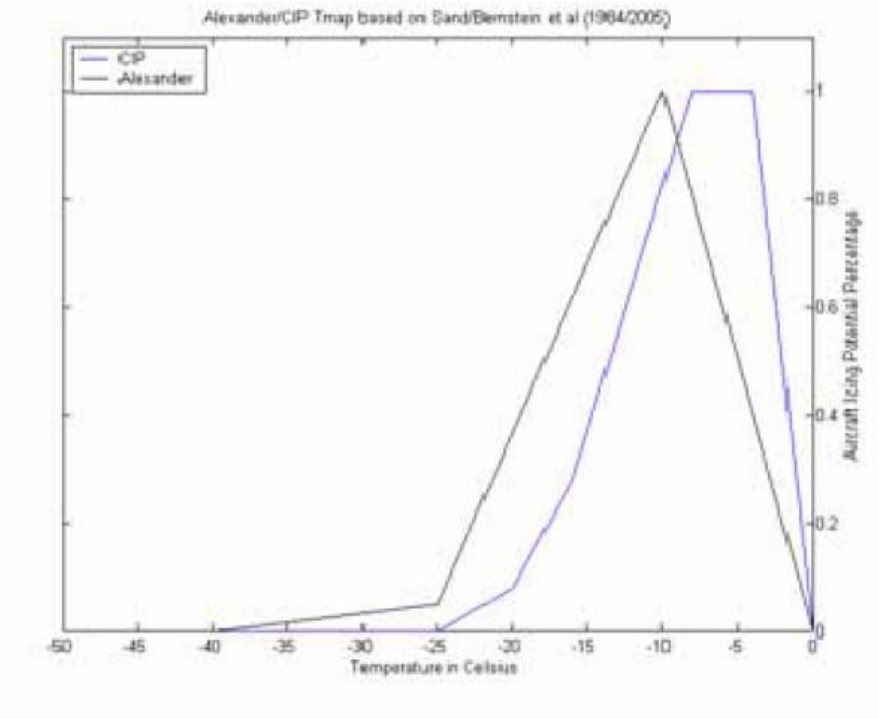

Figure 17. T Interest Map: Icing potential as a function of temperature (black = From Alexander 2005 and blue = From Bernstein et al. 2005)

III. PROCEDURE

The original idea for this study was to collect model data from storms transiting the northeastern United States during late spring into early summer. Unfortunately the storms did not produce adequate icing for this study. However, historical NOGAPS and COAMPS data stored on the GODAE server at http://www.usgodae.org/cgi-bin/datalist.pl?generate=summary was extremely valuable in completing this study. Data from early 2004 was used since it contained some significant icing events and the most complete data sets. The northeastern United States was chosen due to the amount of PIREPS available in that area and is also consistent with the area studied in Alexander (2005) and Cooper (2006). MODIS imagery for the same the same time period was obtained from the National Aeronautics and Space Administration (NASA) website at http://ladsweb.nascom.nasa.gov/data/search.html. PIREPS were obtained from the National Climatic Data Center (NCDC) website at http://hurricane.ncdc.noaa.gov/pls/plhas/has.dsselect.

A. NOGAPS AND COAMPS MODEL INVESTIGATION

Fleet Numerical Meteorological and Oceanography Center (FNMOC) model data stored on the GODAE server was downloaded in gridded binary (GRIB) format and decoded using the commercially available Integrated Data Viewer (IDV) by Unidata. Using the IDV Temperature, Dewpoint and RH data from the closest level to the available PIREP (typically 850mb) was retrieved and put into an Excel spreadsheet for analysis. The forecast model run that preceded the PIREP time was used, and the data came from the forecast hour closest to the PIREP (i.e., PIREP is 1310 so the 12Z model run would be used and the 1300 data would be used). Figure 18 shows an example of the IDV output of 850mb temperatures over North America.

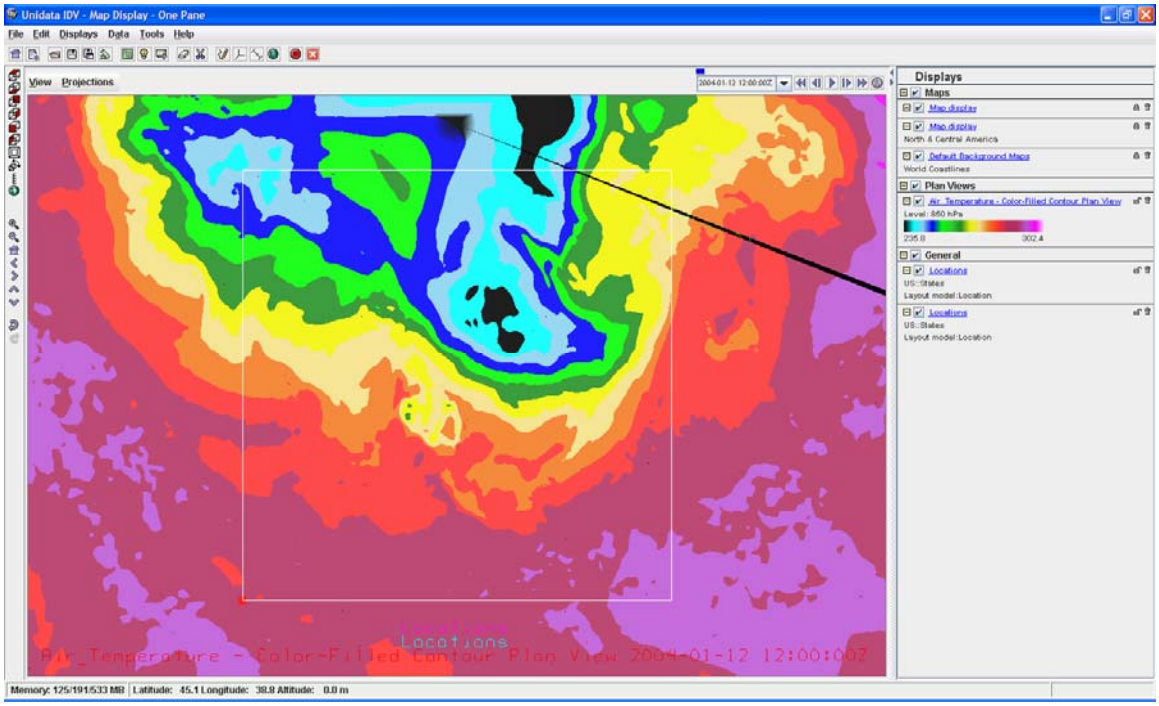

Figure 18. IDV display of 850mb temperatures over North America

Obtaining data from the IDV is quite simple by use of a data probe that allows the user to find the exact data for any latitude and longitude. If the PIREP reported level fell between two model levels, then the two levels were investigated and interpolated if needed. Since RH was one of the model output parameters it was not necessary to calculate RH from the temperature and dewpoint. However RH was calculated from model temperature and dewpoint to insure the model output consistency.

B. MODIS LEVEL 1 DATA INVESTIGATION

Using the MODIS algorithm developed by Alexander (2005), MODIS level-1 data was decoded and compared to the corresponding PIREPS. PIREPS from four hours on either side of the MODIS image were used for comparison. This is a slight change from Cooper (2006) who used only three hours on either side. This change was necessary due to receiving PIREPS from the archive versus real time. There are significantly more PIREPS available in real time that makes it to the archive. In order to have more PIREPS available, the observational time on either side of the PIREP was extended slightly. When

the MODIS image is compared to the PIREPS pixels within 25 miles of the PIREP are examined to determine the mean and median values within that area. The maximum of either the mean or median is used to determine the MODIS icing potential ($MODIS_{pot}$) (Cooper 2006).

C. TOTAL ICING POTENTIAL CALCULATIONS

1. Model Icing Potential Assignment

Temperature and relative humidity are the only two parameters needed for the simplistic model icing potential assignment. Both parameters are available in the model output. Icing potential due to model RH is assigned based on the RH Interest Map (Figure 16). Icing potential due to model T is assigned based on the use of Alexander or CIP T Interest Map (Figure 17). When the MATLAB code is run the user has a choice on which T_{map} is used. For the purpose of this study both T_{map} were used for comparison.

2. Five Test Calculations

Five test calculations using both T_{map} curves were conducted resulting in 10 overall icing potentials. These tests are the same that Cooper (2006) used with the exception of the 1.5 hr difference model forecast which resulted in eight tests in that study. COAMPS is shown, but the same calculations were also used for the NOGAPS data. Cooper (2006) did the same for ETA in his study but did not include the ETA results. These tests are necessary to determine which factor, RH or T, is more important in the icing potential calculation and to determine how much the model data should be weighted compared to the MODIS data. Using both T_{map} curves determines which T_{map} provides the best results. Each variable and calculation is described below and shown in Table 2.

a. Relative Humidity

The RH formula, shown in Table 2, for calculating RH was used in Cooper (2006), but was not needed in this study because it was given in the model output. It was used as a validation tool to insure the T_D model output and RH were in agreement.

b. COAMPS1

COAMPS1 gives equal weighting to T_{pot} and RH_{pot} which are multiplied together and square root taken. The square root result is then multiplied by the $MODIS_{pot}$ and the square root of that gives the icing potential for COAMPS1.

c. COAMPS2

COAMPS2 gives more weighting to Tpot by multiplying it by itself and then multiplying RH_{pot} and taking the cube root. The cube root result is then multiplied by the $MODIS_{pot}$ and the square root of that gives the icing potential for COAMPS2.

d. COAMPS3

COAMPS3 is the same as COAMPS2 except the extra weighting is given to the RH_{pot} by multiplying it by itself and then multiplying T_{pot} and taking the cube root. The cube root result is then multiplied by the $MODIS_{pot}$ and the square root of that gives the icing potential for COAMPS3.

e. COAMPS4

COAMPS4 simply weights $MODIS_{pot}$ by 60% and COAMPS3 by 40%.

f. COAMPS5

COAMPS5 takes COAMSP3 result multiplied by the $MODIS_{pot}$ and the square root of that is the icing potential of COAMPS5. Cooper (2006) used this calculation due to the favorable results of the similar COAMPS3 calculation.

Table 2. COAMPS Model Icing Calculations

Variable	Formula
Relative Humidity (RH)	$RH \approx 100(\frac{112 - 0.1T + T_D}{112 + 0.9T})^8$ (National Weather Service 2005)
Icing Potential Test 1 using T and T_D from closest forecast hour (COAMPS1)	$COAMPS1 = \sqrt{(\sqrt{T_{pot} * RH_{pot}}) * MODIS_{pot}}$ (Cooper 2006)
Icing Potential Test 2 (COAMPS2)	$COAMPS2 = \sqrt{(\sqrt[3]{T_{pot} * T_{pot} * RH_{pot}}) * MODIS_{pot}}$ (Cooper 2006)
Icing Potential Test 3 (COAMPS3)	$COAMPS3 = \sqrt{(\sqrt[3]{T_{pot} * RH_{pot} * RH_{pot}}) * MODIS_{pot}}$ (Cooper 2006)
Icing Potential Test 4 (COAMPS4)	$COAMPS4 = 0.6 * MODIS_{pot} + 0.4 * COAMPS3$
Icing Potential Test 5 (COAMPS5)	$COAMPS5 = \sqrt{COAMPS3 * MODIS_{pot}}$

D. VERIFICATION

To provide a direct comparison with Cooper (2006), a similar verification system was used that followed from Alexander (2005). If the PIREP location had a 0.4 value or greater it was considered high icing potential while less than 0.4 was considered low icing potential. Using these potential values they were compared with the actual positive and negative PIREPS to determine which ones were correctly identified. Alexander (2005) and Cooper (2006) used a 0.5 threshold, but after analyzing data for this study a threshold of 0.4 was determined to be a better fit for the data in this study.

From the above results, the probability of detection (POD), also known as sensitivity, can be calculated by taking the total number of correctly identified positive PIREPS divided by the total number of positive PIREPS. The probability of detection null (POD_{no}), also known as specificity, is calculated in a similar manner by taking the number of correctly identified negative PIREPS divided by the total number of negative PIREPS (Cooper 2006). The results are discussed in the next chapter.

IV. RESULTS

Cooper (2006) used receiver operating characteristic curves (ROC), which are simply a graphical plot of sensitivity versus one minus specificity, for presentation of his MODIS and MM5 data. For comparison, similar data styles and ROC curves are provided in this study. ROC curves are good for data that can be identified as true or false, which is the case for identifying positive or negative PIREPS. Icing probabilities from the MODIS icing algorithm and the model icing algorithm are compared to the historic PIREPS to determine whether the icing is correctly identified. An icing probability of 0.4 or greater compared to a positive PIREP will yield a true result while an icing probability of 0.4 or greater compared to a negative PIREP will yield a false positive. The inverse is also true; an icing probability of less than 0.4 compared to a positive PIREP will yield a false negative while an icing probability of less than 0.4 compared to a negative PIREP will yield a true result. Accuracy is calculated by taking the number of positive or negative PIREPS identified correctly divided by the total number of PIREPS. Sensitivity is the number of correctly identified positive PIREPS divided by the total number of positive PIREPS. Specificity is the number of correctly identified negative PIREPS divided by the total number of negative PIREPS.

A. ALEXANDER T_{MAP}

As stated earlier, there are two distinctive T_{map} maps available for calculating icing probability. The first one used for model data output is the Alexander T_{map} that is shown in Figure 17 as a solid black line. Using a commercially available ROC curve program, jrocfit.org, the MODIS and model icing probability data was input along with the PIREPS and the resulting data is shown in Table 3. Along with the accuracy, sensitivity and specificity discussed above, the empirical ROC area is the area below and to the right of the ROC curves which means the curves with the highest area should provide the best results, but that is not always the case. If the data has a lot more of either positive or negative cases the data may be artificially skewed. This is the case for the data in this study because of the lack of available negative PIREPS. The associated ROC

curves from Table 3 are shown in Figure 19. The best possible ROC curve would be a straight line from 0 on the x-axis to the 1 on the y-axis. This means that curves that are tilted closer to the y-axis are generally better.

Table 3. Calculation Results for PIREPS using Alexander T_{map}

Calculation	Accuracy (%)	Sensitivity (%)	Specificity (%)	Empirical ROC Area
MODIS	58.8	57.1	66.7	0.476
COAMPS1	64.7	67.9	50.0	0.568
COAMPS2	61.8	64.3	50.0	0.554
COAMPS3	73.5	82.1	33.3	0.580
COAMPS4	58.8	57.1	66.7	0.637
COAMPS5	58.8	57.1	66.7	0.637
NOGAPS1	82.4	89.3	50.0	0.613
NOGAPS2	79.4	85.7	50.0	0.583
NOGAPS3	82.4	89.3	50.0	0.619
NOGAPS4	55.9	57.1	50.0	0.563
NOGAPS5	58.8	57.1	66.7	0.649

1. ROC Curves Using Alexander T_{map}

Looking at Table 3 above and Figure 19 below, one can see that the best ROC curve is NOGAPS5 which is the furthest to the left and has the highest ROC area. While scientifically NOGAPS5 is the best result from the ROC process, the lack of negative PIREPS, which was also a problem for Alexander (2005) and Cooper (2006), artificially skews the results. Since the data is skewed, the data should be examined in more detail in the tabular format.

There were six times as many positive PIREPS compared to negative PIREPS so one of the most significant results is the sensitivity. A high sensitivity means the positive PIREPS were properly identified. The MODIS calculation had one of the lowest sensitivities coming in just under 60%. The COAMPS1 calculation that weights temperature and humidity equally increased the sensitivity to just under than 70%. The T-weighted COAMPS2 reduced to a sensitivity of around 65%. The COAMPS3 sensitivity which weights RH more gives the highest sensitivity for the COAMPS group at just over 80%. COAMPS4 and COAMPS5 which use different weighting of the COAMPS3 field are very similar to the MODIS field by itself with a sensitivity value just under 60%. The NOGAPS fields had a similar trend with NOGAPS1 producing a sensitivity of just under 90%. NOGAPS2, similar to COAMPS2, reduced slightly to a sensitivity of around 85%. NOGAPS3 had one of the highest sensitivities for the NOGAPS group, just like COAMPS3 for the COAMPS group, with a sensitivity value just below 90%. NOGAPS4 and NOGAPS5 decrease significantly to a sensitivity value just below 60%.

Based on high sensitivity values, NOGAPS1, NOGAPS3, NOGAPS2 and COAMPS3 provide the best results. Heavier weighting of RH also produced the best results for Cooper (2006). Even though the number of negative PIREPS makes them statistically insignificant, the NOGAPS group identified at least 50% or more negative PIREPS correctly. The COAMPS group did the same with the exception of COAMPS3 which only correctly identified 33% of the negative PIREPS. This gives the edge for accurately predicting icing to the NOGAPS group, specifically the equally weighted NOGAPS1 and the RH-weighted NOGAPS3.

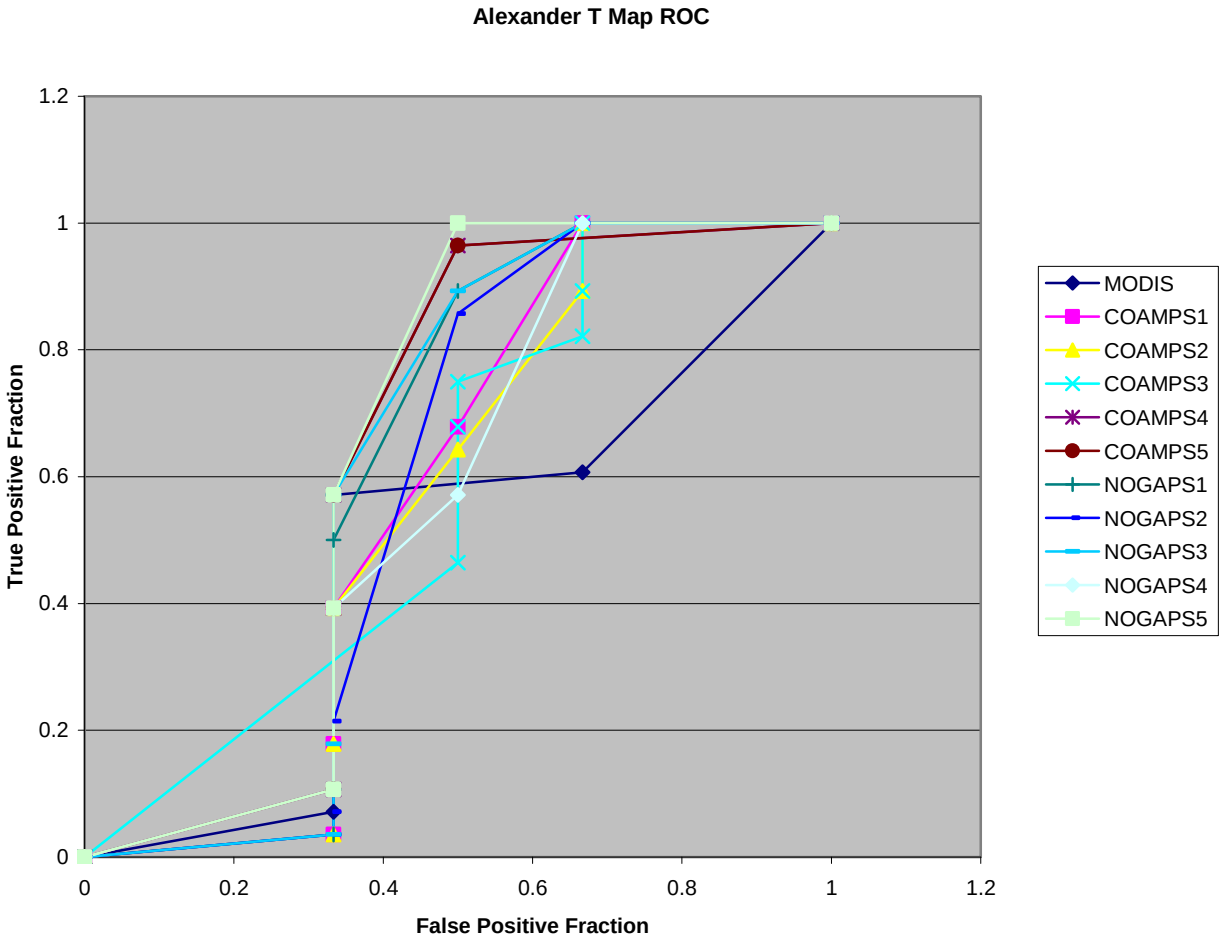

Figure 19. ROC curves for MODIS and model icing potentials using Alexander Tmap

B. CIP T_{MAP}

The CIP T_{map} is shown as the solid blue line in Figure 17. The CIP T_{map} assigns a higher icing probability over a broader range of temperatures and the ROC curve results are shown in Table 4 below. Contrary to the data results in Cooper (2006), the accuracies and sensitivities for the CIP T_{map} were either better or at least the same as the Alexander T_{map}. The associated ROC curves for the CIP T_{map} are shown in Figure 20 below.

Table 4. Calculation Results for PIREPS using CIP Tmap

Calculation	Accuracy (%)	Sensitivity (%)	Specificity (%)	Empirical ROC Area
MODIS	58.8	57.1	66.7	0.476
COAMPS1	91.2	96.4	66.7	0.696
COAMPS2	73.5	75.0	66.7	0.667
COAMPS3	85.3	92.9	50.0	0.667
COAMPS4	58.8	57.1	66.7	0.625
COAMPS5	58.8	57.1	66.7	0.637
NOGAPS1	91.2	96.4	66.7	0.679
NOGAPS2	91.2	96.4	66.7	0.679
NOGAPS3	88.2	96.4	50.0	0.646
NOGAPS4	58.8	57.1	66.7	0.637
NOGAPS5	58.8	57.1	66.7	0.649

1. ROC Curves Using CIP T_{map}

Looking at table 4 above and Figure 20 below one can see the best ROC curve is NOGAPS1. Unlike the Alexander T_{map} where the results were skewed by the lack of negative PIREPS the lack of negative PIREPS did not have as great of an effect on the CIP T_{map} results. The MODIS calculation did not change from the Alexander T_{map} and has a sensitivity of just under 60%. COAMPS1 which has the highest ROC area also has the highest sensitivity with a value just over 95%. The COAMPS2 calculation reduces about 20% and has a sensitivity value around 75%. COAMPS3 increased about 20% and has a sensitivity of just over 90%. COAMPS4 and COAMPS5 share sensitivities with the MODIS value of just under 60%. The NOGAPS fields start off strongly with NOGAPS1,

NOGAPS2 and NOGAPS3 each having sensitivities of just over 95%. NOGAPS4 and NOGAPS5, just like their equals in the COAMPS group, share the MODIS sensitivity of just under 60%.

COAMPS1, NOGAPS1, NOGAPS2 and NOGAPS3 produced the best results respectively. Unlike the Alexander T_{map} calculations where the specificities dropped below 50% none of the CIP T_{map} calculations reach that level. All of the calculations correctly identify 2 out of 3 negative PIREPS with the exception of COAMPS3 and NOGAPS3 which only reach the 50% level. The calculation for COAMPS1 and NOGAPS1 weights T and RH equally which is significant since Cooper (2006) found weighting RH more to be crucial in that study and was an important factor for the Alexander T_{map} results in this study. This shows that where the model output T lies on the T_{map} plays a very important role in the results. If several of the T model data points lie in the 0 to -10 region as they did for this study that can have significant impact on the results when they are weighted heavier over a broader region as is the case for the CIP T_{map}. Just like the Alexander T_{map} the edge for correctly identifying icing goes to the NOGAPS group with the same score for the equally weighted NOGAPS1 and the T-weighed NOGAPS2.

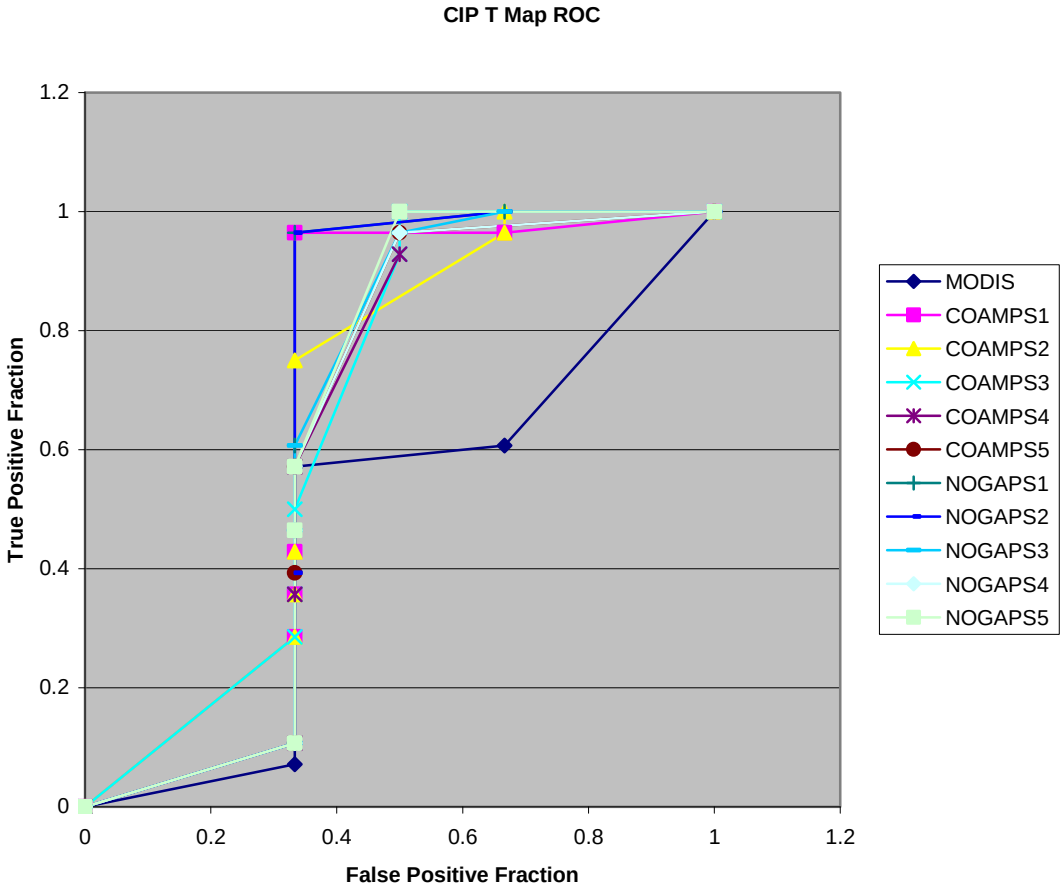

Figure 20. ROC curves for MODIS and model icing potentials using CIP Tmap

THIS PAGE INTENTIONALLY LEFT BLANK

V. CONCLUSION AND RECOMMENDATIONS

A. CONCLUSION

In a perfect world the results of this study would have meshed perfectly with the findings of Cooper (2006). Unfortunately, this is not the case and this study revealed different findings. The first major difference is that the threshold for detecting icing was lowered to 40% vice the 50% used by Alexander (2005) and Cooper (2006). Several thresholds were evaluated and 40% clearly produced the best results for both the MODIS and model icing algorithms. Alexander (2005) and Cooper (2006) suggest looking at some variations in the icing threshold, but there is insufficient explanation for why 50% was chosen. Due to this slight variation between theses, this threshold should be examined for all models and the MODIS icing algorithm. The second major difference compared to Cooper (2006) is the better performance of the CIP T_{map} compared to the Alexander T_{map}. This can be attributed to many of the temperatures being in the range where the CIP T_{map} has a broad range of high icing potentials. The third difference was related to the weighting of the T and RH. In Cooper (2006), weighting RH did a better job of identifying the icing areas. While that was the case to some extent with the Alexander T_{map} and CIP T_{map}, in this study the CIP T_{map} equal weighting of T and RH produced the best results for the COAMPS group and one of the best for the NOGAPS group.

NOGAPS beat out COAMPS for both T_{map} test groups, and this is not a surprise since icing is predominantly a synoptic scale event, but it should be noted that mesoscale factors such as very mountainous terrain like what is experienced in Afghanistan could have a significant impact on icing development. Another shortcoming of this study is the lack of available PIREPS especially negative PIREPS. While there were sufficient positive PIREPS to show some statistical significance the lack of negative PIREPS skewed the ROC analysis. While it can be seen that the COAMPS and NOGAPS model data enhance the detection of icing when combined with the MODIS data, it is not clear on how discriminatory the product is. Without being able to verify that the algorithm is

adequately identifying non-icing areas it is difficult to call it a total success, yet I do believe there is some operational usefulness in this product. Even in its limited form it could be another tool for an operational commander or forecaster to make an informed icing potential forecast.

The armed forces' method of hatching out an area on a map and saying there is going to be icing within the hatched area is not a very useful operational tool. An operational commander trying to make an informed decision about whether the mission can succeed or not should be supplied with probabilistic information vice an either on or off deterministic approach. This combined model and MODIS algorithm product is a stepping stone in developing such a probabilistic product. Already in development is an ensemble model that is capable of a probabilistic icing product. With this new ensemble forecast, combined with the MODIS algorithm the icing forecast product can be greatly improved.

B. RECOMMENDATIONS

The first recommendation would be to continue this study based on the new ensemble model that is being developed. A model capable of producing a probabilistic product along with the MODIS algorithm that can produce a probabilistic output would be very beneficial to military planners. It would not be a far reach to continue this study on volumetric data vice just point sources. Integrating the data both horizontally and vertically could produce a 3-D picture to help the forecaster or military planner to visualize the situation. With a visualization tool it might be easier to see what is needed to mitigate the icing potential. Developing a 3-D picture with model data will not be difficult, but some complexities arise with the MODIS algorithm due to the limitations of looking through the entire cloud. Another limitation to this approach is verifying the extent of icing or lack of icing throughout the volume since PIREPS only provide point source information. This could be overcome in a detailed study with an available airplane to verify icing conditions. Another recommendation is to further identify where a forecaster in the loop (FITL) needs to be placed in the process. Where to place the FITL

might change upon changing weather conditions or terrain, but needs to be identified in detail so the FITL is effectively utilized.

With the progression of theses from Alexander (2005), Cooper (2006) and this study there is sufficient background work to attempt a major study that would combine all the previous models used along with the new ensemble model and the MODIS algorithm to determine which model performs best under several conditions. There are several obstacles to be overcome such as increasing the availability of PIREPS to verify icing and setting the study up over a sufficient length of time to cover multiple icing situations. Mesoscale effects such as mountainous areas need to be looked at to see if that has a significant impact on the icing product. Due to the complexity of this problem, it is highly recommended that a PhD student complete this study.

THIS PAGE INTENTIONALLY LEFT BLANK

LIST OF REFERENCES

Air Safety Foundation, 2002: Safety Advisor, Weather No. 1: Aircraft Icing. Federal Aviation Administration.

Alexander, J. B., 2005: Enhancement of the daytime GOES-based aircraft icing potential algorithm using MODIS. M.S. Thesis, Dept. of Meteorology, Naval Postgraduate School, Monterey, CA.

Bernstein, B.C., F. McDonough, M.K. Politovich, B.G. Brown, T.P. Ratvasky, D.R. Miller, C.A. Wolff and G. Cunning, 2005: Current Icing Potential (CIP): Algorithm description and comparison with aircraft observations. *J. Appl. Meteor*., 44, 969-986.

Cooper, M. J., 2006: Enhancement of the daytime MODIS based aircraft potential algorithm using mesoscale model data. M.S. Thesis, Dept. of Meteorology, Naval Postgraduate School, Monterey, CA.

GODAE COAMPS Archive – Fleet Numerical Meteorology and Oceanography Center, cited 2007: COAMPS 2004 GRIB Data. [Available online at http://usgodae3.fnmoc.navy.mil/ftp/outgoing/fnmoc/models/coamps/conus/2004/], accessed August 2007.

GODAE NOGAPS Archive – Fleet Numerical Meteorology and Oceanography Center, cited 2007: NOGAPS 2004 GRIB Data. [Available online at http://usgodae3.fnmoc.navy.mil/ftp/outgoing/fnmoc/models/nogaps/2004/], accessed August 2007.

Hearn, J. T., 2007. Lear 45 Icing. [Available online at http://www.flickr.com/photos/jthearn/368991194/in/set-72157594331921097/], accessed March 2007.

Kilian, M., 2001: Experimental warbirds pull combat duty. *Chicago Tribune*, November 8.

MODIS Data Retrieval – NASA/Goddard Space Flight Center, cited 2007: LAADS Web, MODIS Level 1 and Atmosphere Archive and Distribution Center. [Available online at http://ladsweb.nascom.nasa.gov/data/search.html], accessed August 2007.

PIREPS Data Archive – NOAA Satellite and Information Service, cited 2007: HDDS Access System. [Available online at http://hurricane.ncdc.noaa.gov/pls/plhas/has.dsselect], accessed August 2007.

The National Center for Atmospheric Research, cited 2002: In-Flight Icing. [Available online at http://www.rap.ucar.edu/asr2002/a-icing/a-inflight_icing.htm], accessed January 2007.

THIS PAGE INTENTIONALLY LEFT BLANK

INITIAL DISTRIBUTION LIST

1. Defense Technical Information Center
   Ft. Belvoir, Virginia

2. Dudley Knox Library
   Naval Postgraduate School
   Monterey, California

3. Philip Durkee
   Naval Postgraduate School
   Monterey, California

4. Kurt Nielsen
   Naval Postgraduate School
   Monterey, California